Evolution of Co/Cu multilayer conductivity during growth: An *ab initio* study

P. Zahn,[1] N. Papanikolaou,[2] F. Erler,[1] and I. Mertig[2]
[1]*Technische Universität Dresden, Institut für Theoretische Physik, D-01062 Dresden, Germany*
[2]*Martin-Luther-Universität Halle-Wittenberg, Fachbereich Physik, Fachgruppe Theoretische Physik, D-06099 Halle, Germany*
(Received 17 September 2001; published 25 March 2002)

We present *ab initio* calculations for the in-plane conductivity of Co/Cu multilayer slabs. The electronic structure of the multilayer slabs is calculated by means of density-functional theory within a screened Korringa-Kohn-Rostoker scheme. Transport properties are described using the Boltzmann equation in relaxation-time approximation. We study the change of the conductivity during growth of the multilayer, and we can reproduce the anomalous, non-Ohmic behavior observed experimentally in several multilayer systems. Our results show that this behavior can be explained in terms of the electronic structure of the slab only. No extra assumption for the scattering at the interfaces is necessary. The connection of electronic structure and conductivity during layer-by-layer growth is elucidated by analyzing the layer-projected conductivities.

DOI: 10.1103/PhysRevB.65.134432 PACS number(s): 75.70.Pa, 73.21.−b, 73.61.At

I. INTRODUCTION

The understanding of the size-dependent conductivity in thin-film multilayers is still an open question. The conductivity of various magnetic/nonmagnetic multilayer systems[1–6] has been measured as a function of the thickness of the deposited layer. These electrical measurements were made simultaneously by *in situ* conductance monitoring, and the experimental data show characteristic features for all investigated multilayers. First of all, the conductance increases with increasing multilayer thickness. Second, the slope of the conductance increase is different for the different metal layers, due to the corresponding residual resistivity of the metals. Third, there is a characteristic drop in the total conductance as soon as the magnetic layer is added on top of the nonmagnetic layer. This behavior is quite general and was originally related to additional scattering in the interface region due to intermixing and disorder.

Several models have been developed to understand the origin of this behavior. Most of them have assumed free-electron behavior within the constituent layers,[7–9] extending the Fuchs-Sondheimer approach.[10,11] Disorder at the interface was introduced. A quantum-mechanical description including surface scattering was presented by Fishman and Calecki[12,13] and by Trivedi and Ashcroft.[14] A more realistic description of the multilayer was based on a tight-binding model including disorder at the interface.[1] *Ab initio* electronic structure calculations of magnetic multilayers have been performed by several groups.[15–19] It was shown that the electronic structure of the multilayer plays a very important role for the understanding of the transport properties and giant magnetoresistance.[20,21] None of the calculations were performed for the *in situ* conductance monitoring considering the incremental conductance contributed by each atomic layer. The aim of this work is the understanding of the size dependence and the evolution of the Co/Cu multilayer conductivity during the growth, starting from *ab initio* electronic structure calculations.

II. COMPUTATIONAL APPROACH

The calculations are based on density-functional theory in the local-density approximation and a recently implemented version of a screened Korringa-Kohn-Rostoker Green's-function method.[18,22–25] For layered systems the advantage of this transformation is the N-scaling behavior (with N the number of layers in the system) which enables us to treat systems with a large number of atoms in the unit cell and arbitrary two-dimensional (2D) or three-dimensional cell periodicity. The potentials were assumed to be spherically symmetric inside the Wigner-Seitz sphere as in the atomic sphere approximation (ASA) but a multipole expansion of the charge density has been taken into account up to $l_{max}=6$ (angular momenta up to $l_{max}=3$ have been used for the wave functions). For the exchange-correlation functionals the expressions given by Vosko, Wilk, and Nusair[26] were used. Brillouin-zone integrations have been performed by means of special points methods.[27] To simulate the *in situ* conductance monitoring of the Co/Cu multilayer during growth we model the system by the following assumptions. We consider a monolayer growth along the (001) direction. Co and Cu are assumed to occupy an ideal fcc lattice with a lattice constant of 6.76 a.u., without any lattice mismatch or distortion at the interfaces and surfaces, while no intermixing at the interfaces is allowed.

In the experimental setup an insulator or semiconductor buffer or target material is used; this is simulated by vacuum in our calculation. That means a free standing slab with 2D periodicity in plane is considered. For the calculations we started from a Cu slab of 2 monolayers (ML) thickness. Cu was added layer by layer until a thickness of 5 ML is reached, which corresponds to about 9 Å. We continue by adding Co up to the same thickness. Thus the cycle was repeated. The short hand notation for the considered systems is $\mathrm{Cu}_{n_1}/\mathrm{Co}_{n_2}/\mathrm{Cu}_{n_3}\ldots$ denoting the individual layer thicknesses in monolayers starting from the bottom Cu layer. Every multilayer corresponds to an experimental film after deposition of a complete ideally flat atomic layer. The electronic structure was determined self-consistently for each

system under consideration. Concerning the magnetic configuration of the multilayer slabs we assumed parallel alignment of the Co layer magnetization which is energetically preferred in Co/Cu multilayers[28] with 5 ML Cu thickness.

III. TRANSPORT THEORY

To calculate the electrical conductivity of the considered layered structures we use the semiclassical Boltzmann theory in relaxation-time approximation.[16,29] A spin-independent isotropic relaxation time τ is assumed. This is of course a rough approximation which concentrates on the anisotropic electronic structure of the system but, as our results show, it is sufficient for the explanation of the effect. Moreover, considering that the anisotropic scattering would change our results only quantitatively, and not qualitatively, it thus serves our current purpose of understanding the conductivity of thin multilayers based on the electronic structure of ideal systems. Neglecting spin-flip scattering, Mott's two-current model can be used.[30] With these simplifications the in-plane conductivity σ in relaxation-time approximation is given by a Fermi-surface integral over the in-plane component of the Fermi velocity $v_{\mathbf{k}}^s$ squared,[29]

$$\sigma = \frac{e^2}{4\pi^2\hbar}\tau \sum_s \int d^2\mathbf{k}\, \delta(E_{\mathbf{k}}^s - E_F) v_{\mathbf{k}}^{s\,2}. \tag{1}$$

$E_{\mathbf{k}}^s$ are the energy eigenvalues and E_F is the Fermi level. s denotes the spin directions. The k integration is performed over the two-dimensional Brillouin zone of the slab. The Fermi surface reduces to a set of closed lines in the plane perpendicular to the growth direction (see Fig. 4 below). The result of Eq. (1) is a slab conductivity per unit cell for a two-dimensional system. If we consider only one monolayer then we obtain a conductivity per atom which compares directly to the bulk conductivity.

The wave functions $\Psi_{\mathbf{k}}^s(\mathbf{R}_i + \mathbf{r})$ of the one-electron eigenstates are normalized to the volume of the unit cell. Splitting up the real-space integral into a sum over the atomic spheres, a site-dependent probability amplitude $P_{\mathbf{k}}^s(i)$ of the eigenstate $E_{\mathbf{k}}^s$ is defined,

$$1 = \int_{\text{unit cell}} d^3\mathbf{r} |\Psi_{\mathbf{k}}^s(\mathbf{r})|^2 \tag{2}$$

$$= \sum_i \int_{ASA_i} d^3\mathbf{r} |\Psi_{\mathbf{k}}^s(\mathbf{R}_i + \mathbf{r})|^2 = \sum_i P_{\mathbf{k}}^s(i). \tag{3}$$

$\mathbf{R}_i$ are the basis vectors, denoting the different atomic layers, while the real-space integration in Eq. (3) is restricted to the atomic sphere of atom i (ASA_i).

To analyze the spatial distribution of the current a local conductivity is introduced by projecting the conductivity on each atomic layer i:

$$\sigma_i^s = \frac{e^2}{4\pi^2\hbar}\tau \int d^2\mathbf{k}\, \delta(E_{\mathbf{k}}^s - E_F) v_{\mathbf{k}}^{s\,2} P_{\mathbf{k}}^s(i). \tag{4}$$

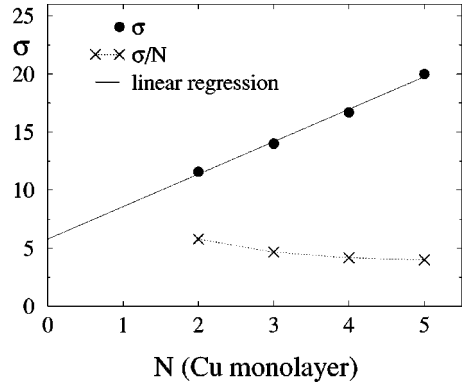

FIG. 1. Film conductivity (dots) and conductivity per atom (crosses) as a function of Cu layer thickness in arbitrary units.

Thus the total conductivity is just the sum over all the layers N of the slab, and spin directions,

$$\sigma = \sum_s \sum_{i=1}^{N} \sigma_i^s. \tag{5}$$

IV. ULTRATHIN CU FILM

Following the ideas of Fuchs and Sondheimer[10,11] the conductivity of a simple metallic film goes to zero with decreasing film thickness D, since in the limit of thin films $\sigma \sim \kappa \ln(1/\kappa)$, where $\kappa = D/l$, and l denotes the mean free path. Considering no diffusive surface scattering we obtain the bulk conductivity. In a realistic quantum-mechanical calculation where full band-structure effects are present the situation is more complicated. In Fig. 1 we present the calculated conductivity of ultrathin Cu slabs with thicknesses varying from two to five monolayers. The total slab conductivity increases almost linearly with the number of Cu monolayers. The conductivity per atom saturates to a constant value after 4–5 ML. It is obvious that our calculated conductivity does not extrapolate to zero as predicted by the Sondheimer model. This is a direct consequence of the quantum-mechanical treatment of the surface. In the Sondheimer model the surface is described by the classical electron distribution function. In the present calculation the full quantum-mechanical Hamiltonian for the surface is used. As a result, types of eigenstates like surface states could appear which are not included in the Sondheimer model. Due to the formation of surface states with a high in-plane group velocity the conductivity per atom (Fig. 1) is increased for very thin Cu slabs. It has to be mentioned that the constant relaxation time that is used for all states at the Fermi level might be inaccurate to obtain quantitative information.

V. CONDUCTIVITY OF CU/CO SLABS

Our calculated conductivity of the Cu/Co slabs is shown in Fig. 2, together with the density of states (DOS) at the Fermi level. With our calculation we are able to reproduce the experimentally observed behavior. Our results show an increase with increasing slab thickness, while there is a drop in the slab conductivity of about 20% when the first Co

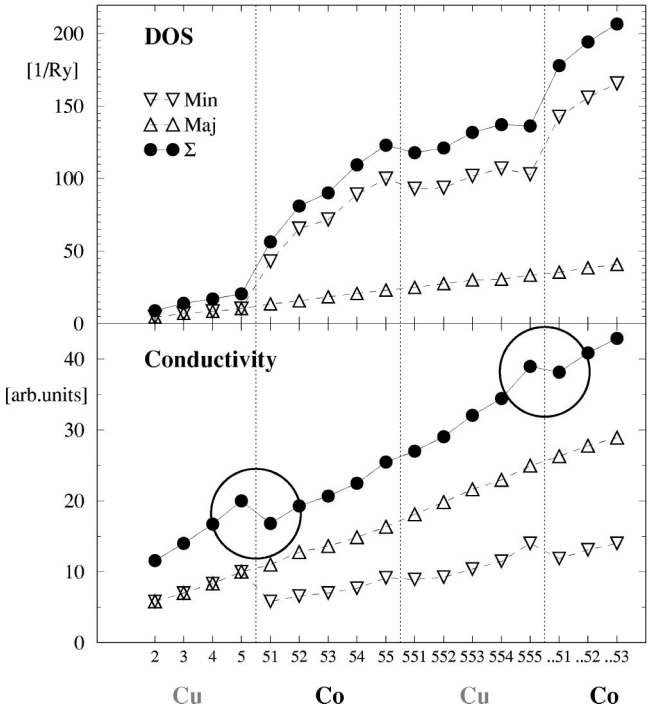

FIG. 2. Evolution of total and spin projected DOS (states/Ry) at E_F and total and spin projected conductivity (arbitrary units) during Co/Cu multilayer growth.

monolayer is deposited on Cu. By adding more Co layers σ increases further, and we observe no significant effect when we start depositing Cu again. A drop is again seen when we repeat the Co deposition on top of Cu. The spin decomposition shows that for majority electrons we have a monotonous increase in σ, while the peculiar, non-Ohmic conductivity variation stems from the minority electrons. Here we point out that no specific surface scattering mechanism is included in the calculation. Moreover, a constant spin-independent relaxation time was assumed, and the difference in the spin channels comes solely from the contrast of electronic structure in the two spin channels while differences in scattering which would require an anisotropic τ are ignored in this approximation.

It is interesting to compare the evolution of the conductivity with the changes of the slab DOS at the Fermi level, shown in Fig. 2. For the majority channel we observe a linear increase with thickness since the local DOS at E_F at the Co and Cu sites is very similar for the majority channel and corresponds to the free-electron-like states above the filled $3d$ bands. The behavior of the minority DOS reflects the difference in the electronic structure of the two materials. The DOS is much larger at the Co sites in comparison to Cu; this causes the strong increase of the total DOS during the Co growth. The local DOS at the Co surface or at a Co/Cu interface is enhanced in comparison to the bulk Co, and the total DOS is strongly increased by adding the first two Co layers. Moreover, quantum confinement effects are fully included in our calculation and cause the reduced increase when depositing the third Co layer, and the small drop when the single Cu layer terminates the slab.

Let us now concentrate on the drop of the conductivity when adding one monolayer of Co on the Cu film. This behavior is accompanied by a strong increase in the total DOS since the Fermi level crosses the Co minority band. The spin projected conductivities demonstrate that the drop occurs in the minority channel. By means of an averaged spin-dependent Fermi velocity $\overline{v^s}$,

$$\overline{v^s}=\left[\int d^2\mathbf{k}\,\delta(E^s_{\mathbf{k}}-E_F)v^{s\,2}_{\mathbf{k}}/n^s(E_F)\right]^{1/2}, \tag{6}$$

one can rewrite Eq. (1) into

$$\sigma=\frac{e^2}{4\pi^2\hbar}\tau\sum_s n^s(E_F)\overline{v^s}^{\,2}. \tag{7}$$

$n^s(E_F)=\int d^2\mathbf{k}\,\delta(E^s_{\mathbf{k}}-E_F)$ is the total DOS at the Fermi level. The expression in Eq. (7) is useful to understand the microscopic origin of the conductivity drop. Following Eq. (7) the reduction of the conductivity is caused by a strong reduction of the averaged Fermi velocity in the minority channel since the DOS is continously increasing. For the majority band we have a linear increase and no difference is seen when going from Cu to Co and vice versa since the Co d states are below the Fermi level. To elucidate this Fermi velocity reduction the local conductivity of the minority channel (Eq. 4) is shown in Fig. 3, for nearly all slabs under consideration. For the pure Cu slabs all Cu layers contribute equally to the conductivity, and we observe only a small reduction at the surface layers. The situation changes drastically when we consider a single monolayer of Co on the Cu slab. As we can see from Fig. 3 (third panel from bottom), the major contribution in the conductivity comes from the Co layers. The Cu contributions, however, are significantly decreased by almost a factor of 4 in comparison to the Cu slabs without Co coverage. According to Eq. (7), this corresponds to a reduction of the effective Fermi velocity by a factor of 2 and the total slab conductivity is decreased (Fig. 2). This reduction of the Fermi velocity stems from a drastic change of the Fermi-surface topology when adding a single Co layer on top of Cu as shown in Fig. 4. The deposition of a simple Co layer destroys the free-electron-like Cu-slab Fermi surface in the minority band while the majority Fermi surface is kept intact. As a result we end up with a complicated minority Fermi surface dominated by Co d states of low velocity (Fig. 4). Despite the low velocity of the Co d states, Co layers have a high σ because of the high DOS. Moreover, Co surface and interface states produce a further enhancement.

The constant reduction of the Cu contribution implies also the experimentally found proportionality of the conductivity drop in dependence on the Cu layer thickness.[1] The conducting states have a large probability amplitude at the surface, which would give an amplification of the conductivity drop due to the enhanced scattering cross section.[31] This is in line with numerical results of Bailey *et al.*[1] assuming a larger potential disorder at the Co/Cu interface in comparison to the bulk materials.

The addition of an extra Cu layer on top of the Co layer is accompanied by a similar conductivity contribution like in the first Cu stack. In the minority channel there is only a

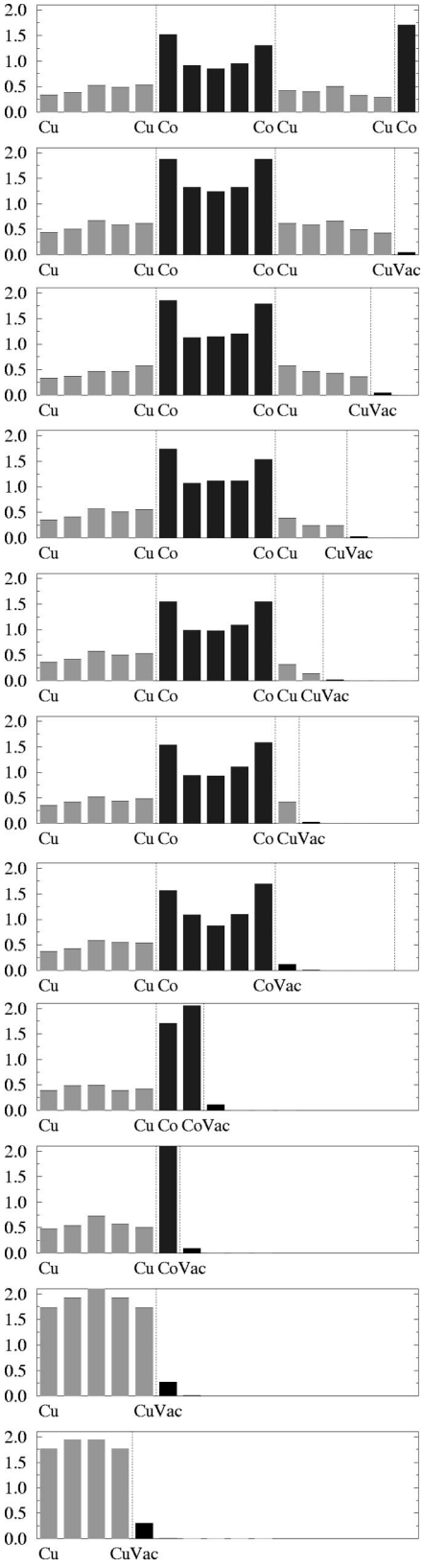

FIG. 3. Evolution of the local conductivity of the minority channel (Eq. 4) (arbitrary units) during film growth.

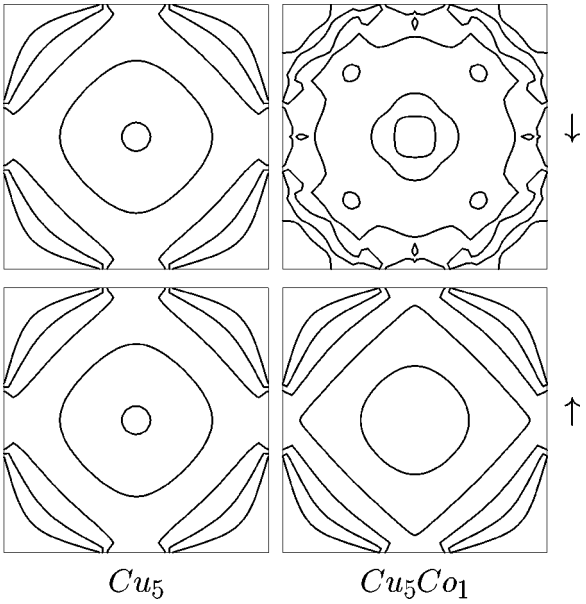

FIG. 4. Fermi surface of Cu_5 and Cu_5Co_1 slabs for minority (upper panel) and majority (lower panel) bands. Note that for $2d$ slabs of finite thickness the Fermi surface reduces to a set of lines.

marginal decrease when we add one monolayer of Cu on top of Co. This is compensated by the linear increase in the majority channel, so that almost no effect is observed in the total σ. With increasing Cu layer thickness a symmetric profile is formed (Fig. 3, second panel from top). The total conductivity increases monotonously. The first Co layer of the second stack causes again a decrease of the underlying Cu layer contributions and a drop of the total σ. The combination of all details in the local conductivity discussed above leads to the observed behavior as a function of the film thickness (Fig. 2), with decreasing conductivity when adding Co on Cu, and a linear increase when adding Cu on Co. The Cu thickness we consider is much smaller compared with the recent experiment of Bailey *et al.*[1] but as we can see from Figs. 1 and 2, a constant conductivity per atom is established after 4–5 ML and larger thickness would only cause a monotonic increase in σ. As mentioned above our calculations are performed for a ferromagnetic configuration of the Co magnetization which is favored by the interlayer distance of 5 ML of Cu. The Cu thickness of 20 Å (11 ML) used in the experiments by Bailey *et al.*[32] and Urbaniak *et al.*[5] corresponds to the second antiferromagnetic maximum of interlayer exchange coupling in Co/Cu and Py/Cu multilayers, respectively. However the actual magnetic configuration of the multilayer slab under consideration was not investigated in the experiments.

The microscopic picture discussed above could be applied to other systems with similar electronic structure, such as Py/Cu,[5] Fe/Ag,[4] and Cr/Au.[2] Depending on the electronic structure of the particular system the role of minority and majority electrons can be changed. The only system that has to be checked in more detail is Cu/Ag.[6] Cu and Ag are isovalent and the band structures are quite similar. The conductivity drop in this system might be related to alloying only.

VI. CONCLUSIONS

Based on *ab initio* calculations of the conductivity of Cu/Co slabs we have shown that the variation during growth can be explained by the changes of the electronic structure as a function of the film thickness. In general the total conductivity of a multilayer slab increases with increasing thickness. A pronounced conductivity drop is obtained when the first Co layer is deposited on top of the Cu. Due to interaction of the Co *d* electrons with the Cu *s* electrons the character of the minority Fermi surface is changed from *sp*- to *d*-like. As a consequence the local conductivity contributions of the Cu layers are reduced. Since the total DOS at the Fermi level increases during film growth the effect is related to reduced Fermi velocities. The microscopic picture can be generalized to any multilayer consisting of noble- and transition-metal layers. This effect is not in contradiction to the conduction drop caused by interface scattering discussed by Bailey *et al.*[32] but can be combined with it. Both effects exist and interface scattering can even amplify the band-structure effects.

[1] W.E. Bailey, S.X. Wang, and E.Y. Tsymbal, Phys. Rev. B **61**, 1330 (2000).
[2] H. Brückl, Ph.D. thesis, Universität Regensburg, 1992.
[3] H. Eckl, G. Reiss, H. Brückl, and H. Hoffmann, J. Appl. Phys. **75**, 362 (1994).
[4] S. Fähler, M. Weisheit, and H.-U. Krebs, Mater. Res. Soc. Symp. Proc. **502**, 139 (1998).
[5] M. Urbaniak, T. Luciński, and F. Stobiecki, J. Magn. Magn. Mater. **190**, 187 (1998).
[6] S. Fähler, M. Weisheit, K. Sturm, and H.-U. Krebs, Appl. Surf. Sci. **154-155**, 419 (2000).
[7] G. Palasantzas and J. Barnaś, Phys. Rev. B **56**, 7726 (1997).
[8] W.A. Harrison, Phys. Rev. B **61**, 7766 (2000).
[9] G. Palasantzas, Y.-P. Zhao, G.-C. Wang, T.-M. Lu, J. Barnaś, and J.Th.M. De Hosson, Phys. Rev. B **61**, 11 109 (2000).
[10] K. Fuchs, Proc. R. Soc. London, Ser. A **34**, 100 (1938).
[11] E.H. Sondheimer, Adv. Phys. **1**, 1 (1952).
[12] G. Fishman and D. Calecki, Phys. Rev. Lett. **62**, 1302 (1989).
[13] G. Fishman and D. Calecki, Phys. Rev. B **43**, 11 581 (1991).
[14] N. Trivedi and N.W. Ashcroft, Phys. Rev. B **38**, 12 298 (1988).
[15] K.M. Schep, P.J. Kelly, and G.E.W. Bauer, Phys. Rev. Lett. **74**, 586 (1995).
[16] P. Zahn, I. Mertig, M. Richter, and H. Eschrig, Phys. Rev. Lett. **75**, 2996 (1995).
[17] W.H. Butler, X.-G. Zhang, D.M.C. Nicholson, T.C. Schulthess, and J.M. MacLaren, Phys. Rev. Lett. **76**, 3216 (1996).
[18] P. Zahn, J. Binder, I. Mertig, R. Zeller, and P.H. Dederichs, Phys. Rev. Lett. **80**, 4309 (1998).
[19] C. Blaas, P. Weinberger, L. Szunyogh, P.M. Levy, and C. Sommers, Phys. Rev. B **60**, 492 (1999).
[20] G. Binasch, P. Grünberg, F. Saurenbach, and W. Zinn, Phys. Rev. B **39**, 4828 (1989).
[21] M.N. Baibich, J.M. Broto, A. Fert, F. Nguyen Van Dau, F. Petroff, P. Etienne, G. Creuzet, A. Friederich, and J. Chazelas, Phys. Rev. Lett. **61**, 2472 (1988).
[22] O.K. Anderson, A.V. Postnikov, and S.Yu. Savrasov, Mater. Res. Soc. Symp. Proc. **253**, 37 (1992).
[23] L. Szunyogh, B. Újfalussy, P. Weinberger, and J. Kollár, Phys. Rev. B **49**, 2721 (1994).
[24] R. Zeller, P.H. Dederichs, B. Újfalussy, L. Szunyogh, and P. Weinberger, Phys. Rev. B **52**, 8807 (1995).
[25] K. Wildberger, R. Zeller, and P.H. Dederichs, Phys. Rev. B **55**, 10 074 (1997).
[26] S.H. Vosko, L. Wilk, and M. Nusair, Can. J. Phys. **58**, 1200 (1980).
[27] H.J. Monkhorst and J.D. Pack, Phys. Rev. B **13**, 5188 (1976).
[28] P. Lang, L. Nordström, K. Wildberger, R. Zeller, P.H. Dederichs, and T. Hoshino, Phys. Rev. B **53**, 9092 (1996).
[29] I. Mertig, Rep. Prog. Phys. **62**, 237 (1999).
[30] N.C. Mott, Adv. Phys. **13**, 325 (1964).
[31] P. Zahn, I. Mertig, R. Zeller, and P.H. Dederichs, Mater. Res. Soc. Symp. Proc. **475**, 525 (1997).
[32] W.E. Bailey, C. Fery, K. Yamada, and S.X. Wang, J. Appl. Phys. **85**, 7345 (1999).